Title: NKG2A inhibition promotes NK cell-CD8^{+} T cell interactions to improve anticancer immunity in ovarian carcinoma

First author: Tereza Lanickova

Corresponding author: Jitka Fucikova

Supplementary Figures

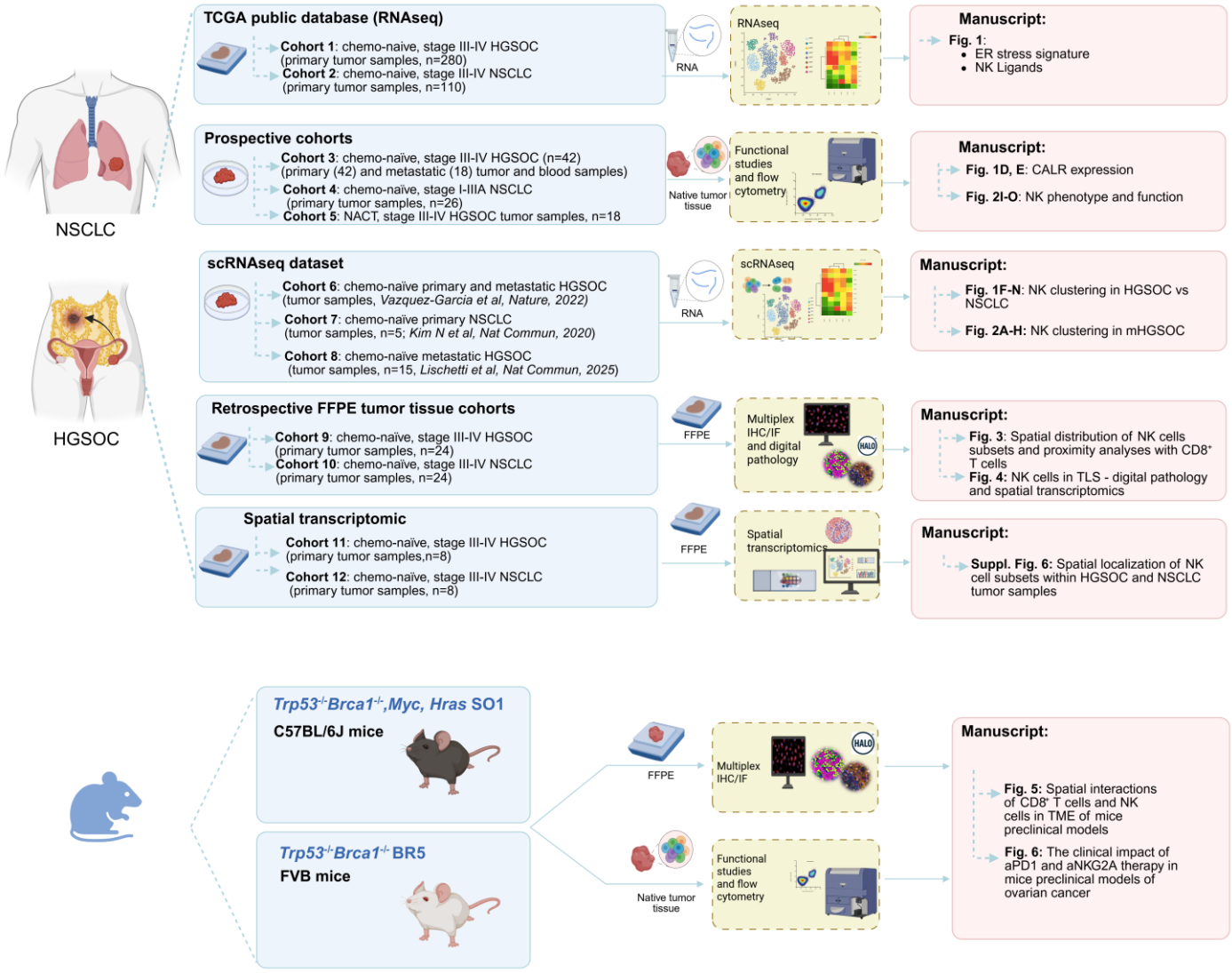

Supplementary Figure 1. **Experimental design of the study.**

Created in BioRender. Palich Fucikova, J. (2026) https://BioRender.com/gxpcmbj.

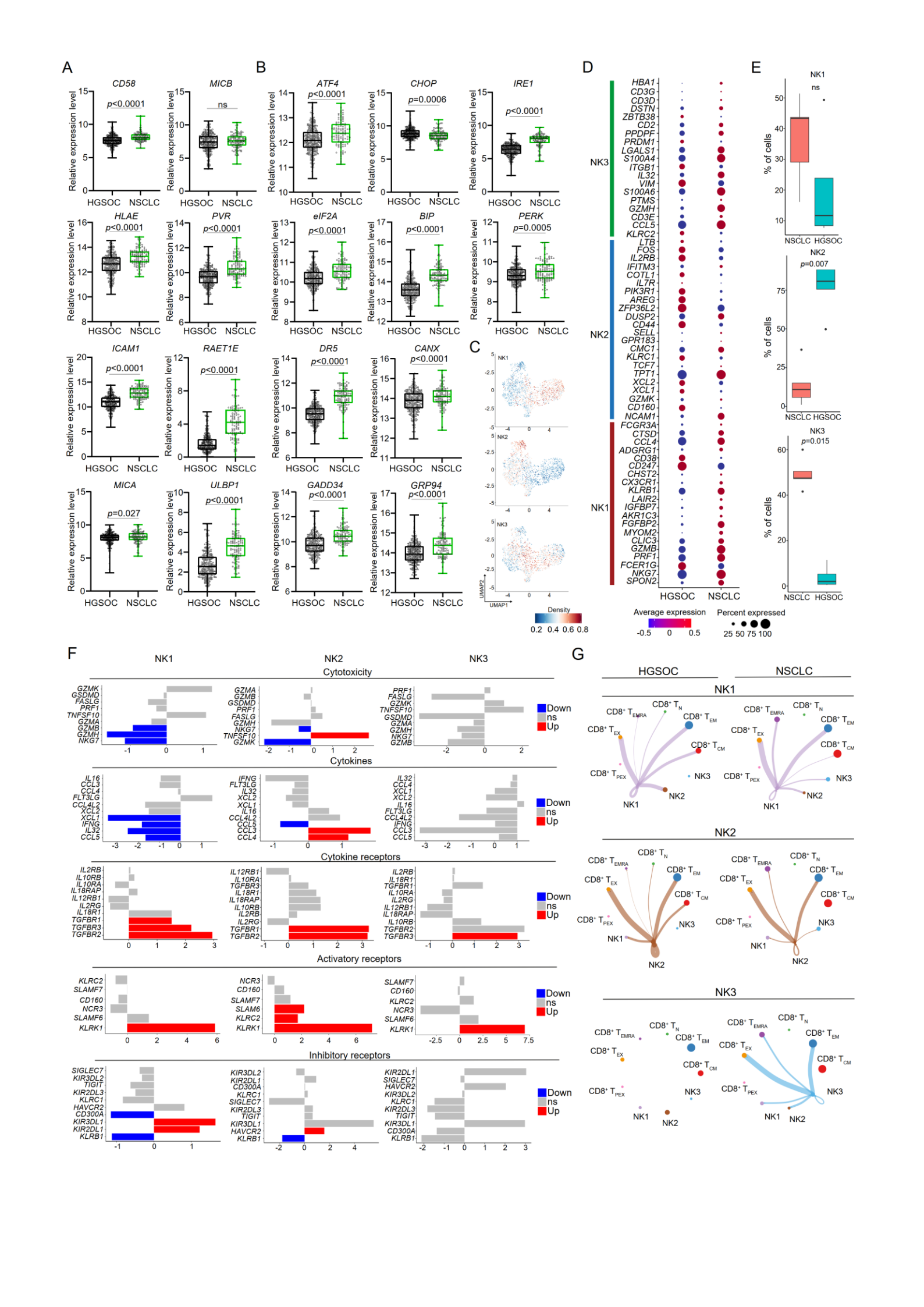
A
B
C
D
E
F
G
CD58
MICB
ATF4
CHOP
IRE1
HLAE
PVR
eIF2A
BIP
PERK
ICAM1
RAET1E
DR5
CANX
MICA
ULBP1
GADD34
GRP94
p<0.0001
ns
p=0.0006
p=0.0005
p=0.027
Relative expression level
HGSOC
NSCLC
NK1
NK2
NK3
UMAP1
UMAP2
Density
HBA1
CD3G
CD3D
DSTN
ZBTB38
CD2
PPDPF
PRDM1
LGALS1
S100A4
ITGB1
IL32
VIM
S100A6
PTMS
GZMH
CD3E
CCL5
KLRC2
LTB
FOS
IL2RB
IFITM3
COTL1
IL7R
PIK3R1
AREG
ZFP36L2
DUSP2
CD44
SELL
GPR183
CMC1
KLRC1
TCF7
TPT1
XCL2
XCL1
GZMK
CD160
NCAM1
FCGR3A
CTSD
CCL4
ADGRG1
CD38
CD247
CHST2
CX3CR1
KLRB1
LAIR2
IGFBP7
AKR1C3
FGFBP2
MYOM2
CLIC3
GZMB
PRF1
FCER1G
NKG7
SPON2
Average expression
Percent expressed
% of cells
p=0.007
p=0.015
F
Cytotoxicity
Cytokines
Cytokine receptors
Activatory receptors
Inhibitory receptors
Down
ns
Up
GZMK
GSDMD
FASLG
PRF1
TNFSF10
GZMA
GZMB
GZMH
NKG7
IL16
CCL3
CCL4
FLT3LG
CCL4L2
XCL2
XCL1
IFNG
IL32
CCL5
IL12RB
IL10RB
IL10RA
IL18RAP
IL12RB1
IL2RG
IL18R1
TGFBR1
TGFBR3
TGFBR2
IL12RB1
IL10RA
TGFBR3
IL18R1
IL18RAP
IL10RB
IL2RB
IL2RG
TGFBR1
TGFBR2
KLRC2
SLAMF7
CD160
NCR3
SLAMF6
KLRK1
SLAM6
SIGLEC7
KIR3DL2
TIGIT
KIR2DL3
KLRC1
HAVCR2
CD300A
KIR3DL1
KIR2DL1
KLRB1
KIR2DL4
KIR2DL5
CD300A
G
HGSOC
NSCLC
CD8+ TN
CD8+ TEMRA
CD8+ TEM
CD8+ TEX
CD8+ TCM
CD8+ TPEX

Supplementary Figure 2. **Enhanced endoplasmic reticulum (ER) stress in NSCLC drives NK cell polarization toward cytotoxic NK1 and NK3 subsets in advanced NSCLC as compared to prominent exhausted NK2 subset in HGSOC.** (A, B) Box plots representing relative expression of genes associated with NK cell stimulatory ligands: *CD58, HLAE, ICAM1, MICA, MICB, PVR, RAET1E, ULBP1* (A) and ER stress signalling: *ATF4, ATF6, BIP*, *CANX, CHOP, EIF2A, GADD34, GRP94, IRE1* and *PERK* (B), determined by RNAseq in chemo-naïve HGSOC (n=280) and NSCLC (n=110) (Cohorts 1 and 2). Box plots: lower quartile, median, upper quartile; whiskers, minimum, maximum. Statistical significance was calculated by two-sided Mann–Whitney U test. *p* values are indicated. (C-E) UMAP (C) and dot plot depicting the 20 most distinguishing genes expressed for NK clusters in HGSOC and NSCLC (Cohorts 6 and 7) (D) and bar plots (E) showing the distribution of NK1, NK2 and NK3 clusters, determined by scRNAseq. Dot size and color encode the percentage of cells within a class, and the average gene expression level, respectively. Mean and SEM are shown. Statistical significance was calculated by two-sided Mann–Whitney U test. *p* values are indicated. (F) Bar plot showing $\log_2$ fold change in genes associated with cytotoxicity, cytokines, cytokine receptors, activating receptors and inhibitory receptors between HGSOC and NSCLC (Cohorts 6 and 7), determined by scRNAseq and analyzed by two-sided Wilcoxon rank-sum test. Bars are coloured according to differential expression significance: red indicates genes significantly upregulated in HGSOC, blue indicates genes significantly downregulated in HGSOC, and grey represents non-significant (NS) changes. Only genes with adjusted *p*-values <0.05 were considered significantly different. The x-axis and y-axis show $\log_2$ fold change values, and gene names, respectively. (G) Circular plots showing cellular interactions between NK1, NK2 and NK3 cells with intratumoral $CD8^+$ T cells states, including central memory (T_{CM}), effector memory (T_{EM}), terminally differentiated (T_{EMRA}), progenitor exhausted (T_{PEX}), exhausted (T_{EX}) and naïve (T_N) in chemo-naïve NSCLC and HGSOC, determined by scRNAseq (Cohorts 6 and 7). Circle size and edge width are proportional to the number of cells in each cell cluster and the communication score between interacting cell clusters.

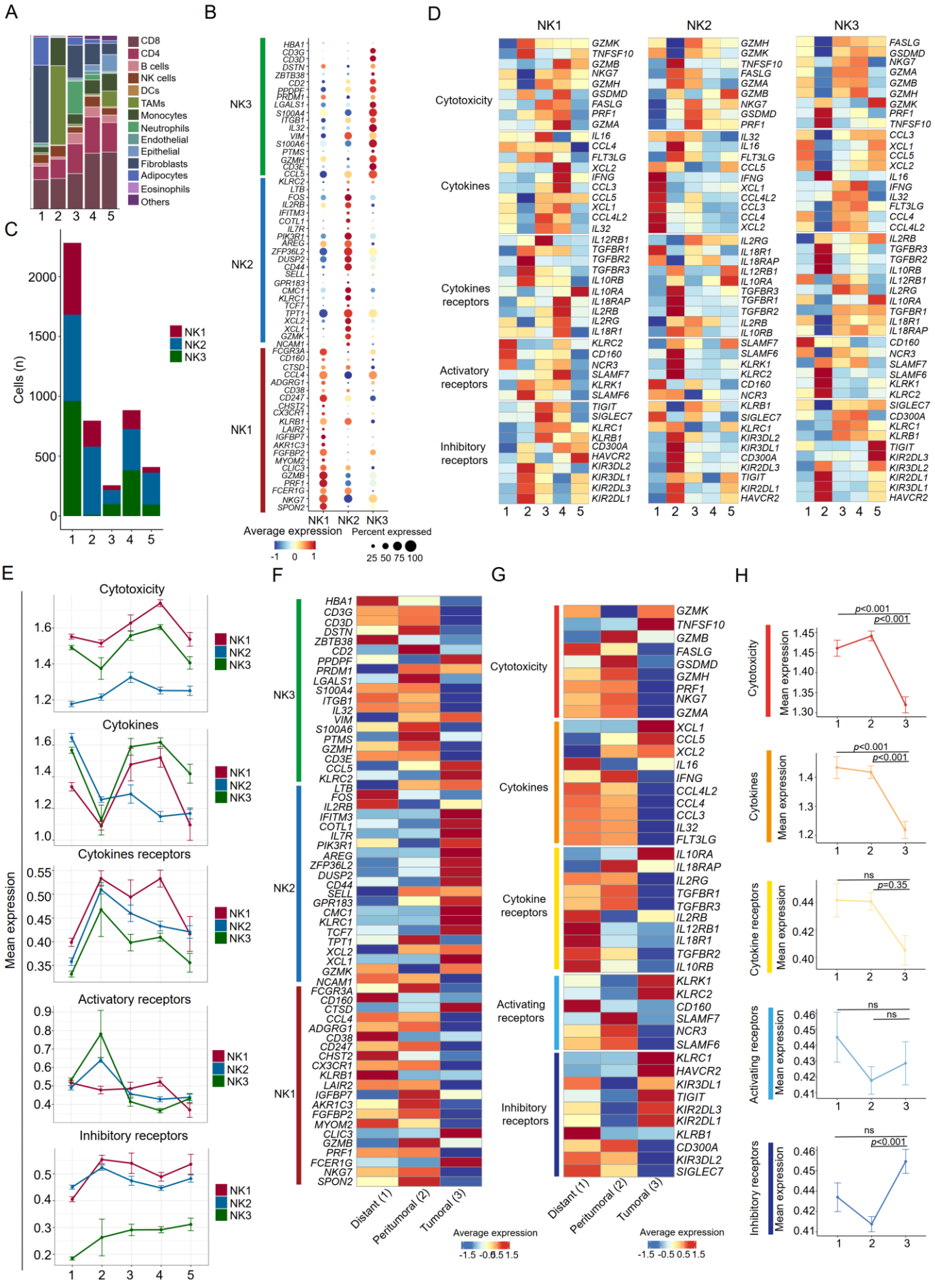
A
CD8
CD4
B cells
NK cells
DCs
TAMs
Monocytes
Neutrophils
Endothelial
Epithelial
Fibroblasts
Adipocytes
Eosinophils
Others
1 2 3 4 5
B
NK3
NK2
NK1
HBA1 CD3G CD3D DSTN ZBTB38 CD2 PPDPF PRDM1 LGALS1 S100A4 ITGB1 IL32 VIM S100A6 PTMS GZMH CD3E CCL5 KLRC2 LTB FOS IL2RB IFITM3 COTL1 IL7R PIK3R1 AREG ZFP36L2 DUSP2 CD44 SELL GPR183 CMC1 KLRC1 TCF7 TPT1 XCL2 XCL1 GZMK NCAM1 FCGR3A CD160 CTSD CCL4 ADGRG1 CD38 CD247 CHST2 CX3CR1 KLRB1 LAIR2 IGFBP7 AKR1C3 FGFBP2 MYOM2 CLIC3 GZMB PRF1 FCER1G NKG7 SPON2
NK1 NK2 NK3
Average expression
-1 0 1
Percent expressed
25 50 75 100
C
Cells (n)
2000
1500
1000
500
0
NK1
NK2
NK3
1 2 3 4 5
D
NK1
NK2
NK3
Cytotoxicity
Cytokines
Cytokines receptors
Activatory receptors
Inhibitory receptors
GZMK TNFSF10 GZMB NKG7 GZMH FASLG PRF1 GZMA
IL16 CCL4 FLT3LG XCL2 IFNG CCL3 CCL5 XCL1 CCL4L2 IL32
IL12RB1 TGFBR1 TGFBR2 TGFBR3 IL10RB IL10RA IL18RAP IL2RB IL2RG IL18R1
KLRC2 CD160 NCR3 SLAMF7 KLRK1 SLAMF6
TIGIT SIGLEC7 KLRC1 KLRB1 CD300A HAVCR2 KIR3DL2 KIR3DL1 KIR2DL3 KIR2DL1
GZMH GZMK TNFSF10 FASLG GZMA GZMB NKG7 GSDMD PRF1
IL32 IL16 FLT3LG CCL5 IFNG XCL1 CCL4L2 CCL3 CCL4 XCL2
IL2RG IL18R1 IL18RAP IL12RB1 IL10RA TGFBR3 TGFBR1 TGFBR2 IL2RB IL10RB
SLAMF7 SLAMF6 KLRK1 KLRC2 CD160 NCR3 KLRB1 SIGLEC7 KLRC1 KIR3DL2 KIR3DL1 CD300A KIR2DL3 TIGIT KIR2DL1 HAVCR2
FASLG GSDMD NKG7 GZMA GZMB GZMH GZMK PRF1 TNFSF10
CCL3 XCL1 CCL5 XCL2 IL16 IFNG IL32 FLT3LG CCL4 CCL4L2
IL2RB TGFBR3 TGFBR2 IL10RB IL12RB1 IL2RG IL10RA TGFBR1 IL18R1 IL18RAP
CD160 NCR3 SLAMF7 SLAMF6 KLRK1 KLRC2 SIGLEC7 CD300A KLRC1 KLRB1 TIGIT KIR2DL3 KIR3DL2 KIR2DL1 KIR3DL1 HAVCR2
1 2 3 4 5
E
Mean expression
Cytotoxicity
Cytokines
Cytokines receptors
Activatory receptors
Inhibitory receptors
NK1
NK2
NK3
1 2 3 4 5
F
NK3
NK2
NK1
HBA1 CD3G CD3D DSTN ZBTB38 CD2 PPDPF PRDM1 LGALS1 S100A4 ITGB1 IL32 VIM S100A6 PTMS GZMH CD3E CCL5 KLRC2 LTB FOS IL2RB IFITM3 COTL1 IL7R PIK3R1 AREG ZFP36L2 DUSP2 CD44 SELL GPR183 CMC1 KLRC1 TCF7 TPT1 XCL2 XCL1 GZMK NCAM1 FCGR3A CD160 CTSD CCL4 ADGRG1 CD38 CD247 CHST2 CX3CR1 KLRB1 LAIR2 IGFBP7 AKR1C3 FGFBP2 MYOM2 CLIC3 GZMB PRF1 FCER1G NKG7 SPON2
Distant (1)
Peritumoral (2)
Tumoral (3)
Average expression
-1.5 -0.5 0.5 1.5
G
Cytotoxicity
Cytokines
Cytokine receptors
Activating receptors
Inhibitory receptors
GZMK TNFSF10 GZMB FASLG GSDMD GZMH PRF1 NKG7 GZMA
XCL1 CCL5 XCL2 IL16 IFNG CCL4L2 CCL4 CCL3 IL32 FLT3LG
IL10RA IL18RAP IL2RG TGFBR1 TGFBR3 IL2RB IL12RB1 IL18R1 TGFBR2 IL10RB
KLRK1 KLRC2 CD160 SLAMF7 NCR3 SLAMF6
KLRC1 HAVCR2 KIR3DL1 TIGIT KIR2DL3 KIR2DL1 KLRB1 CD300A KIR3DL2 SIGLEC7
Distant (1)
Peritumoral (2)
Tumoral (3)
Average expression
-1.5 -0.5 0.5 1.5
H
Cytotoxicity
Cytokines
Cytokine receptors
Activating receptors
Inhibitory receptors
Mean expression
p<0.001
p<0.001
p<0.001
p<0.001
ns
p=0.35
ns
ns
ns
p<0.001
1 2 3

Supplementary Figure 3. **NK cells from advanced HGSOC exhibit transcriptomic signatures of reduced cytotoxicity and increased expression of inhibitory receptors.** (A) Stacked plot of cells passing the quality control, colored by cell type in across (1) benign omentum (n=8), (2) primary tumor (n=5) and omentum with metastases (n=7), comprising three regions: (3) macroscopically tumor-free sites distant to the metastasis, and (4) peritumoral region adjacent to the tumor, as well as (5) chemo-naïve metastatic tumors within the greater omentum (Cohorts 6 and 8). Created in BioRender. (B, C) Dot plot (B) and stacked bar plot (C) of NK1, NK2 and NK3 clusters in 5 histological compartments (described in panel A). (D, E) Heatmap (D) and line plot (E) showing the differential expression of markers of interest among NK cell subsets within 5 histological compartments (shown in panel A). The color scale is based on z-score-scaled gene expression. The z-score distribution ranges from −2 (blue) to 2 (red). (F, G) Heatmaps representing NK cluster distribution (F) and differential expression of markers of interest among NK cell subsets (G) within 3 metastatic omental regions: 1) distant = macroscopically tumor-free sites distant to the metastasis, 2) peritumoral region adjacent to the tumor and 3) chemo-naïve metastatic tumors within the greater omentum (Cohort 8). The color scale is based on z-score-scaled gene expression. The z-score distribution ranges from −2 (blue) to 2 (red). (H) Line plots of gene signatures associated with cytotoxicity, cytokines, cytokine receptors, activating receptors and inhibitory receptors expressed for the entire NK cluster within 3 histological compartments (described in panel A), determined by scRNAseq in Cohort 8. Gene expression was analyzed using the two-sided Wilcoxon rank-sum test with Bonferroni adjustment.

A

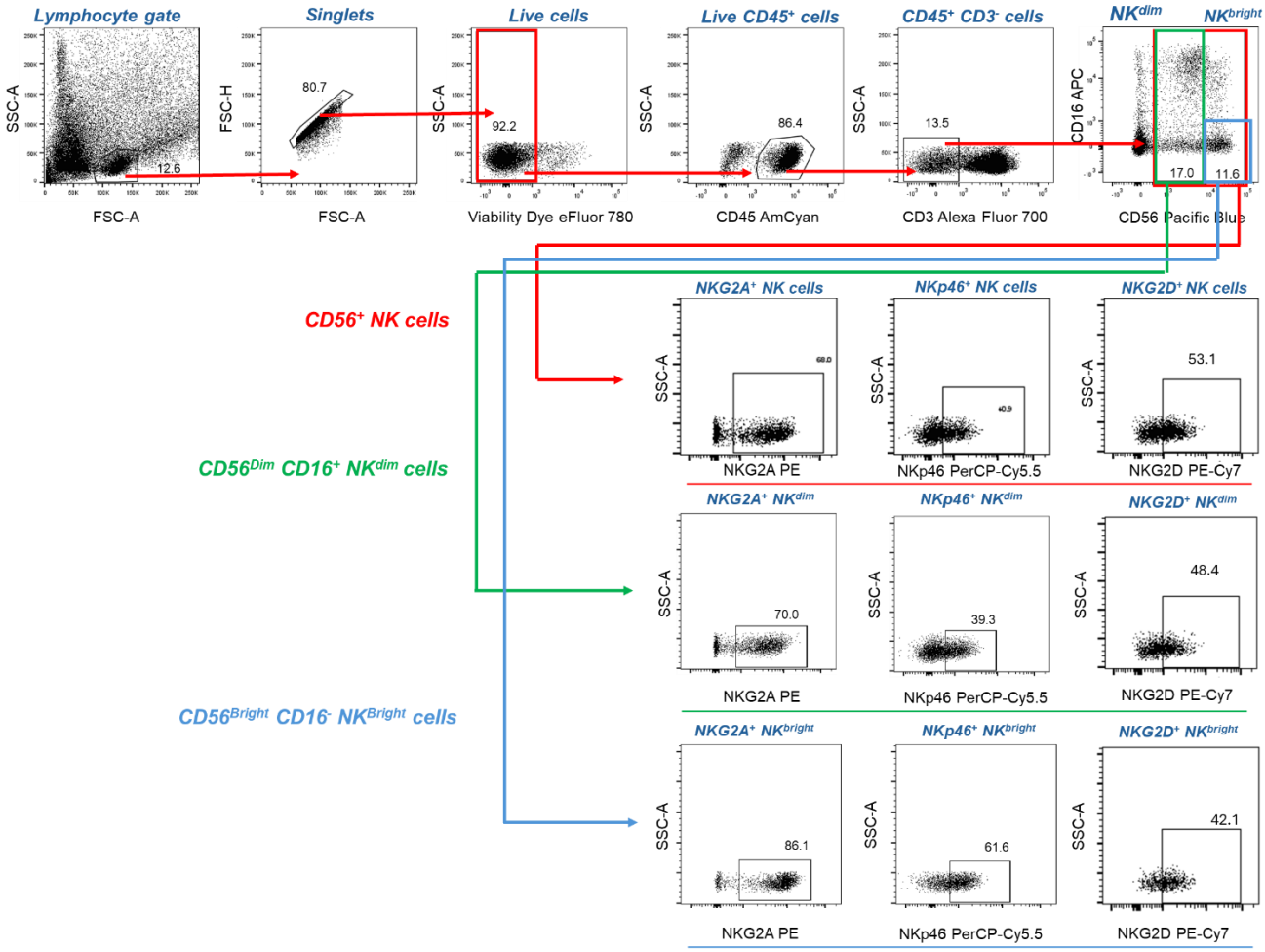
Lymphocyte gate
Singlets
Live cells
Live CD45⁺ cells
CD45⁺ CD3⁻ cells
NKdim
NKbright
SSC-A
FSC-H
FSC-A
80.7
12.6
92.2
86.4
13.5
CD16 APC
17.0
11.6
Viability Dye eFluor 780
CD45 AmCyan
CD3 Alexa Fluor 700
CD56 Pacific Blue
CD56⁺ NK cells
CD56Dim CD16⁺ NKdim cells
CD56Bright CD16⁻ NKBright cells
NKG2A⁺ NK cells
NKp46⁺ NK cells
NKG2D⁺ NK cells
53.1
NKG2A PE
NKp46 PerCP-Cy5.5
NKG2D PE-Cy7
NKG2A⁺ NKdim
NKp46⁺ NKdim
NKG2D⁺ NKdim
70.0
39.3
48.4
NKG2A⁺ NKbright
NKp46⁺ NKbright
NKG2D⁺ NKbright
86.1
61.6
42.1

B

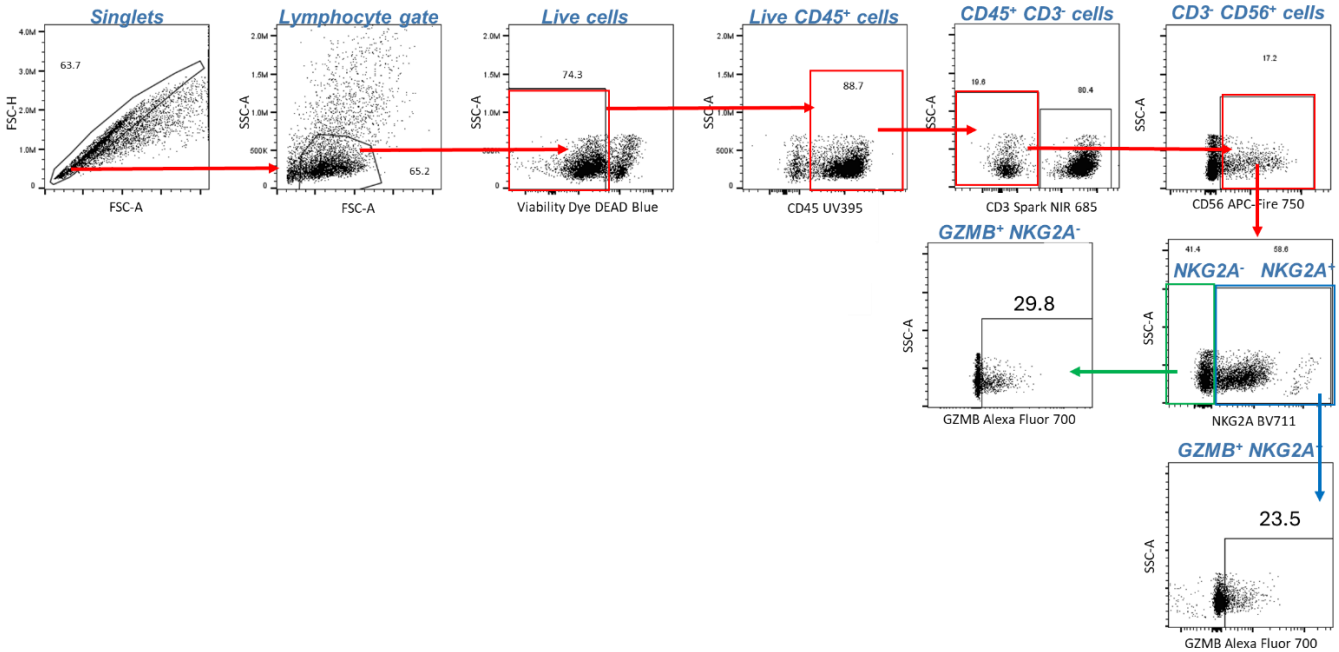
Singlets
Lymphocyte gate
Live cells
Live CD45⁺ cells
CD45⁺ CD3⁻ cells
CD3⁻ CD56⁺ cells
FSC-H
SSC-A
FSC-A
63.7
65.2
74.3
88.7
19.6
80.4
17.2
Viability Dye DEAD Blue
CD45 UV395
CD3 Spark NIR 685
CD56 APC-Fire 750
GZMB⁺ NKG2A⁻
NKG2A⁻ NKG2A⁺
29.8
41.4
58.6
GZMB Alexa Fluor 700
NKG2A BV711
GZMB⁺ NKG2A⁺
23.5

c

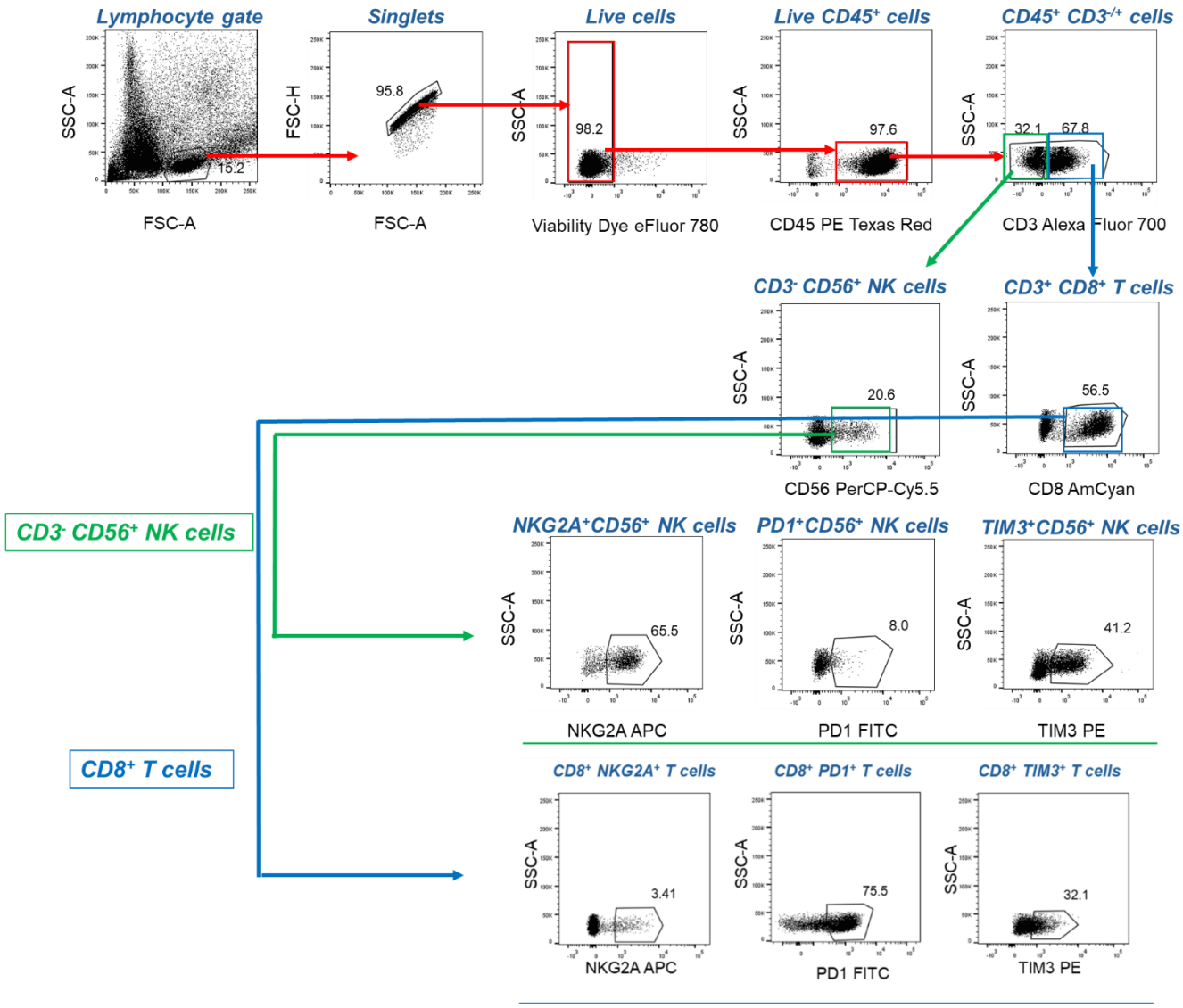

Supplementary Figure 4. **Gating strategy in human tumor samples.** (A) Detection of relative numbers of NKG2A^{+}, NKp46^{+} and NKG2D^{+} CD56^{dim}CD16^{+} NK^{dim} cells, CD56^{bright}CD16^{-} NK^{bright} cells and CD56^{+} NK cells in human tumor samples, determined by flow cytometry. NK cells were identified as live CD45^{+}, CD3^{-} lymphocytes that further expressed CD56 and CD16. This gating strategy supports analyses presented in Fig. 2J-M. (B) Detection of relative numbers of GZMB^{+} NKG2A^{+} *vs* NKG2A^{-} CD56^{+} NK cells. NK cells were identified as live CD45^{+}, CD3^{-} lymphocytes that further expressed CD56. This gating strategy support analyses presented in Fig. 2N. (C) Detection of relative numbers of NKG2A^{+}, PD1^{+} and TIM3^{+} CD45^{+}CD3^{+}CD8^{+} T cells and CD45^{+}CD3^{-}CD56^{+} NK cells in human tumor samples by flow cytometry. NK cells were identified as live CD45^{+}, CD3^{-} lymphocytes that further expressed CD56. This gating strategy support analyses presented in Fig. 2O.

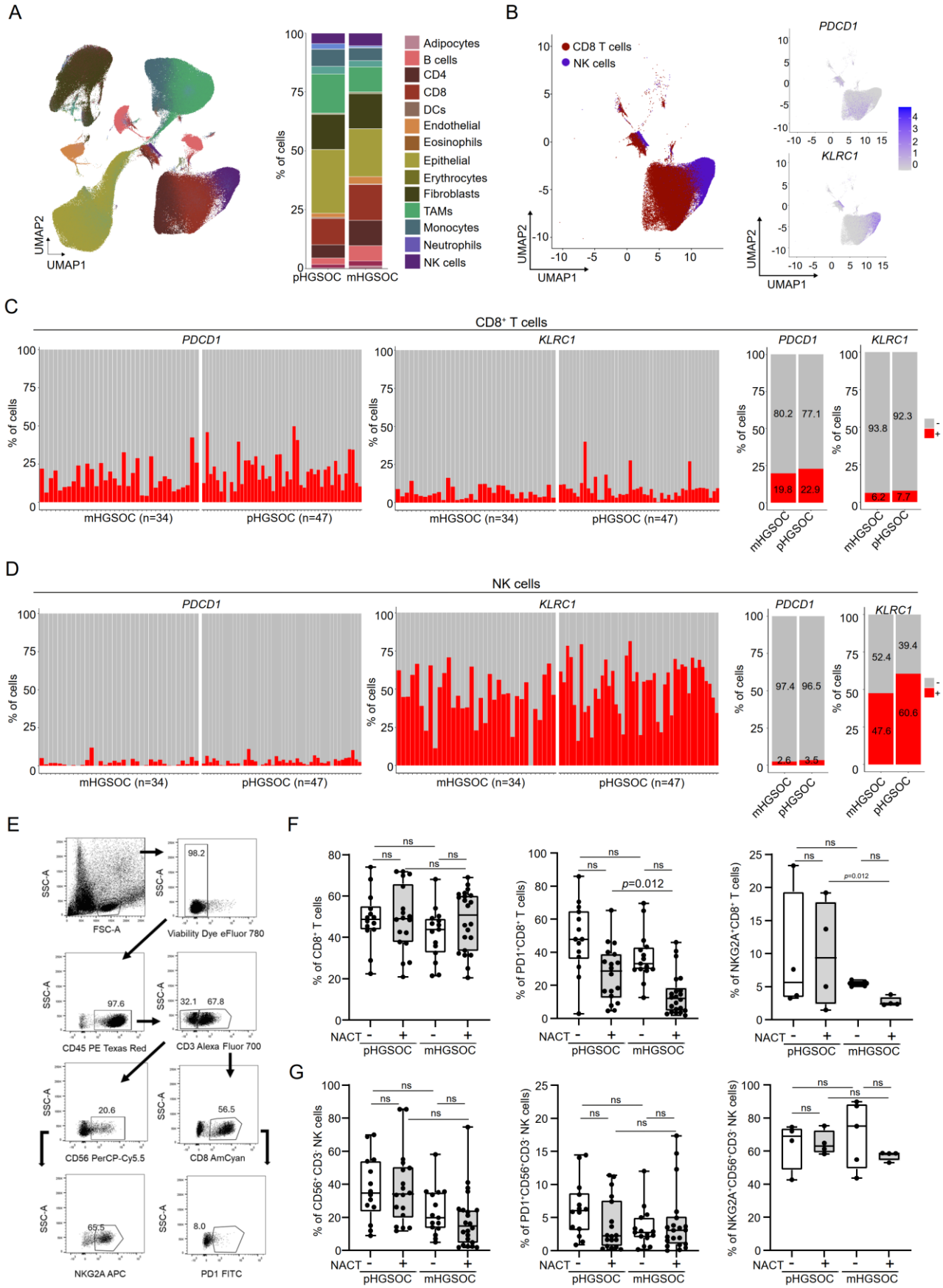

Supplementary Figure 5. **Distribution of PD1⁺ and NKG2A⁺ CD8⁺ T cells and natural killer (NK cells) in chemo-naïve and neoadjuvant chemotherapy (NACT) treated primary and metastatic HGSOC samples.** (A) UMAP and stack plot of cells (n=38,675) passing the quality control, coloured by cell type. (B)

UMAP and stacked plot showing expression of *PDCD1* and *KLRC1* expression in $CD8^+$ T cells and NK-cell clusters in primary (pHGSOC) (n=47) and metastatic HGSOC (mHGSOC) (n=34) samples, determined by scRNAseq (Cohort 6). (C, D) Proportion of $CD8^+$ T cells (C) and NK cells (D) expressing *PDCD1* and *KLRC1* in pHGSOC and mHGSOC, determined by scRNAseq (Cohort 6). (E-G) Representative dot plot (E) and box plots showing flow cytometry analyses quantifying intratumoral $CD8^+$ T cells, $PD1^+CD8^+$ and $NKG2A^+CD8^+$ T cells (F) and intratumoral $CD56^+CD3^-$ NK cells, $PD1^+CD56^+CD3^-$ and $NKG2A^+CD56^+CD3^-$ NK cells (G) within chemo-naïve (n=15) and NACT-treated (n=18) pHGSOC and mHGSOC (Cohorts 3 and 5). Box plots: lower quartile, median, upper quartile; whiskers, minimum, maximum. Statistical significance was calculated by two-sided Mann–Whitney U test. p values are indicated.

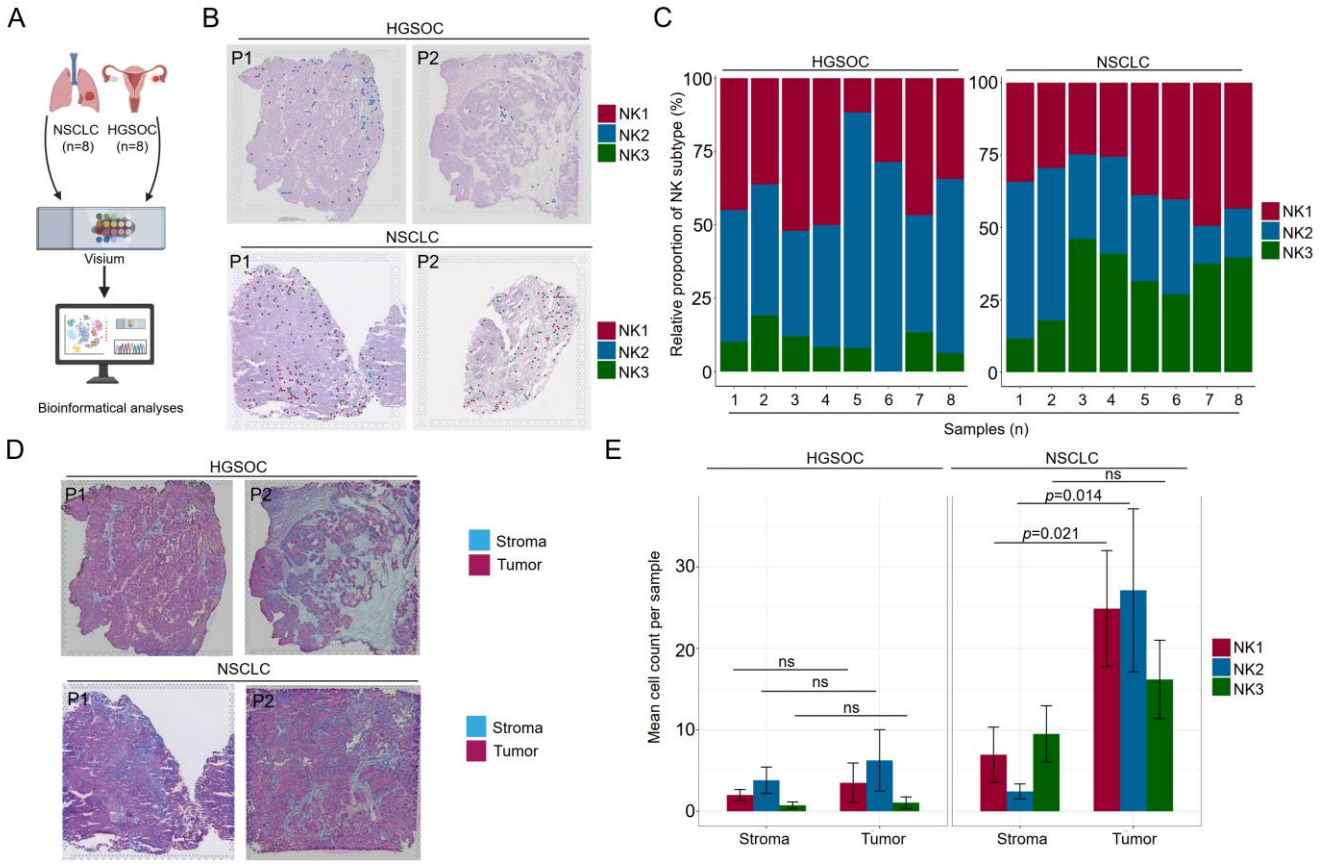

Supplementary Figure 6. **Spatial organization of NK cell subsets within HGSOC and NSCLC.** (A) Experimental workflow in chemo-naïve HGSOC (n = 8) and NSCLC (n = 8) (Cohorts 11 and 12). Spatial transcriptomics was performed on FFPE tumor specimens using the Visium *in situ* platform. Created in BioRender. Palich Fucikova, J. (2026) https://BioRender.com/oc1e9mo. (B-E) Representative spatial maps (B), stacked plots (C), annotation of stroma and tumor core (D) and bar plots (E) showing NK1, NK2, and NK3 cells distribution within tumor core and stromal regions of HGSOC and NSCLC samples. Mean and SEM are shown. Statistical significance was calculated by the two-sided Mann–Whitney U test and the two-tailed Wilcoxon signed-rank test. *p* values are indicated.

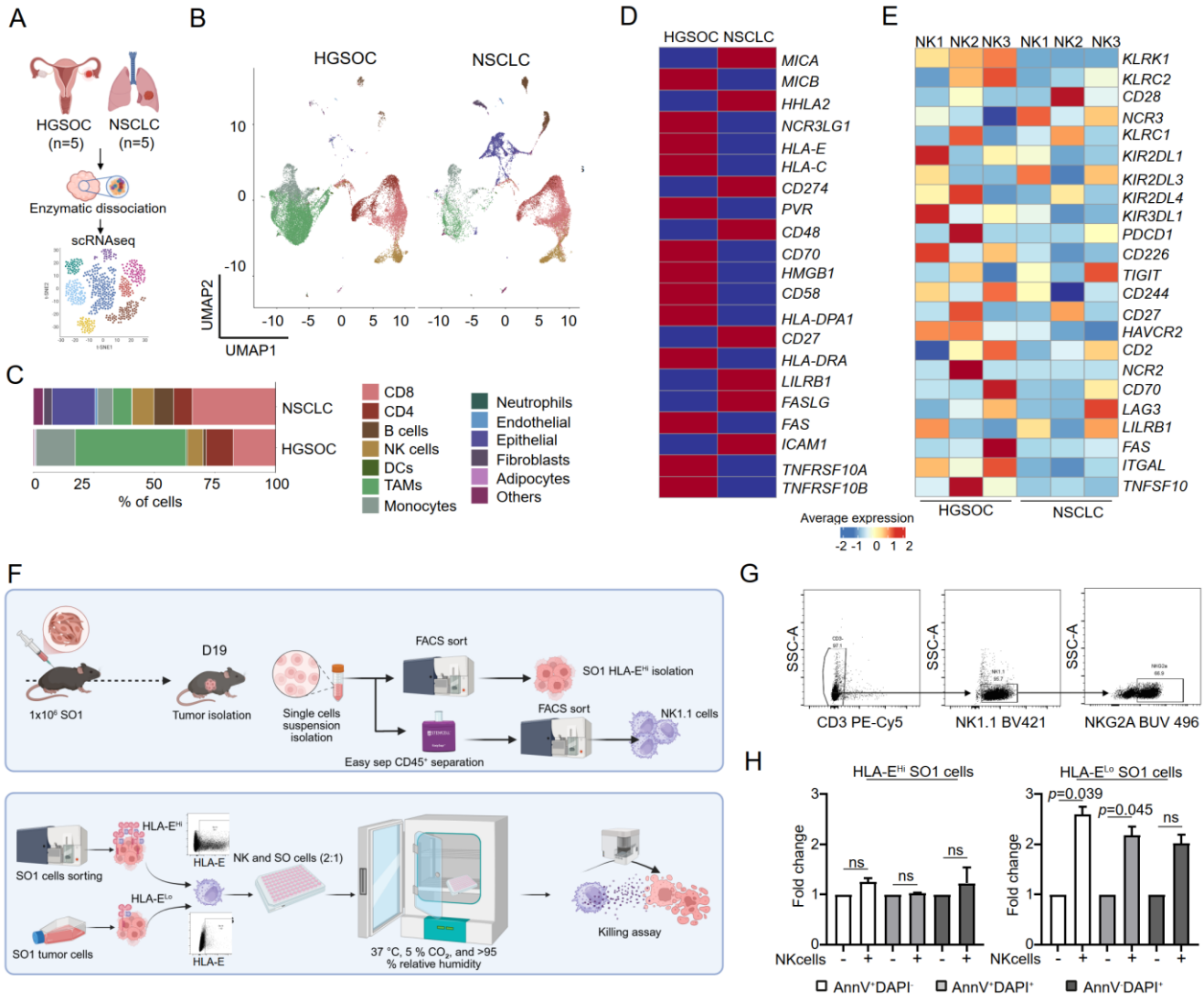

Supplementary Figure 7. **NKG2A–HLA-E axis as a therapeutic checkpoint in HGSOC.** (A) Experimental workflow of scRNAseq on tumor samples of HGSOC (n = 5) and NSCLC (n = 5) patients (Cohorts 6 and 7). Created in BioRender. Palich Fucikova, J. (2026) https://BioRender.com/kr26vkn. (B, C) UMAP and stacked plot of cells passing quality control, coloured by cell type. (D, E) Heatmaps showing differential expression of NK ligands in epithelial clusters (D) and corresponding NK receptors across NK cell subsets in HGSOC and NSCLC (E), shown in panel A. Expression values are z-score scaled. (F) Experimental workflow for NK cell killing assay using the SO1 preclinical ovarian cancer model. NK1.1^{+} cells were isolated from SO1 tumors by FACS. SO1 cell line (HLA-E^{Lo}) and primary SO1 cells (HLA-E^{Hi}) were used as target cells. Created in BioRender. Palich Fucikova, J. (2026) https://BioRender.com/jr4tdf1. (G) Representative dot plot showing purity and NKG2A expression of isolated NK1.1^{+} cells from SO1 tumors. (H) Bar plot showing percentage of early (AnnV^{+}/DAPI^{-}) and late apoptotic (AnnV^{+}/DAPI^{+}), and necrotic (AnnV^{-}/DAPI^{+}) SO1 cells with low versus high HLA-E expression after incubation with NK1.1^{+} cells, determined by flow cytometry. Statistical significance was calculated by two-sided paired t-test; *p* values indicated.

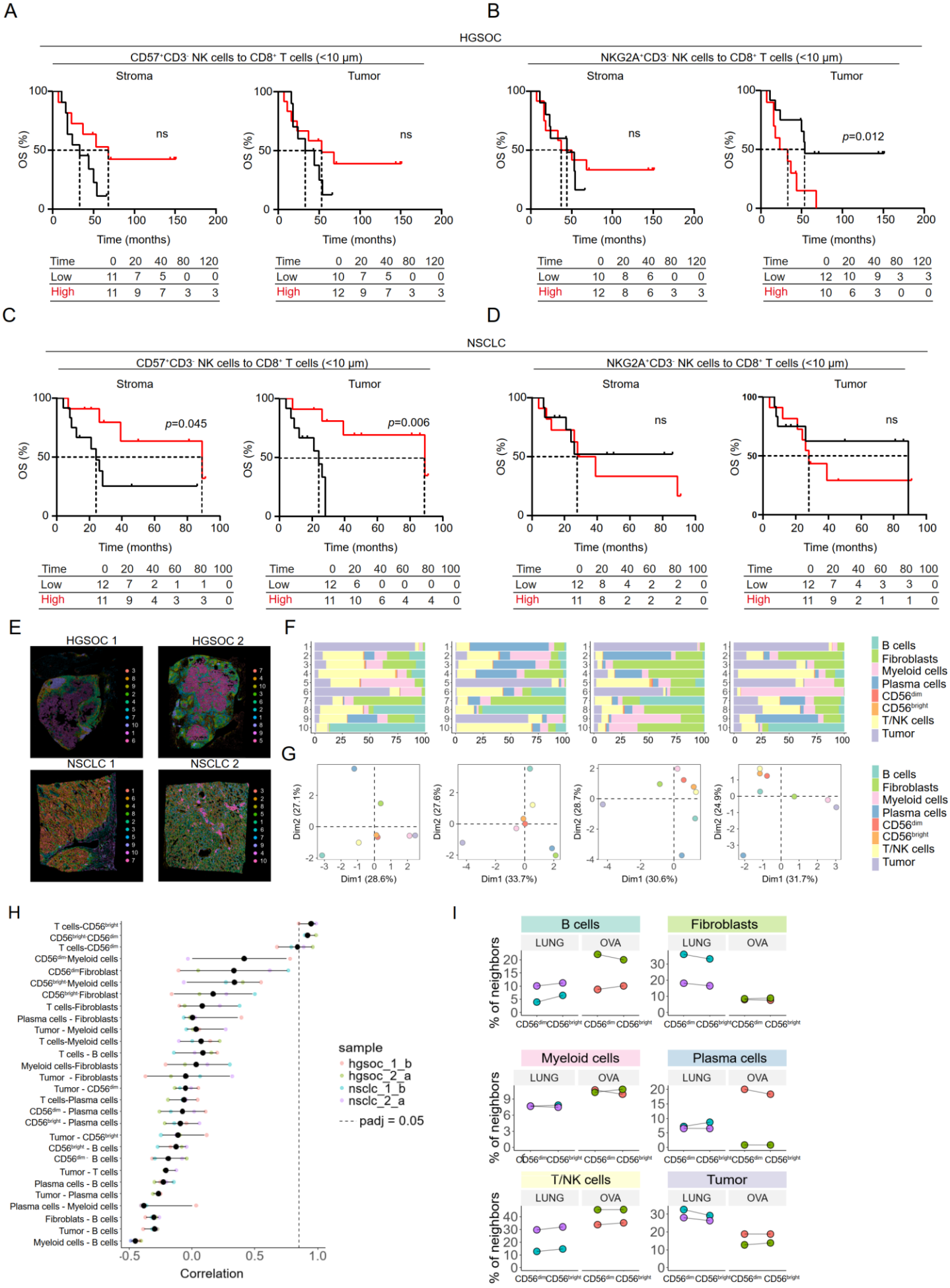
A
B
HGSOC
CD57+CD3- NK cells to CD8+ T cells (<10 μm)
Stroma
Tumor
NKG2A+CD3- NK cells to CD8+ T cells (<10 μm)
OS (%)
Time (months)
ns
p=0.012
Time 0 20 40 80 120
Low 11 7 5 0 0
High 11 9 7 3 3
Low 10 7 5 0 0
High 12 9 7 3 3
Low 10 8 6 0 0
High 12 8 6 3 3
Low 12 10 9 3 3
High 10 6 3 0 0
C
D
NSCLC
p=0.045
p=0.006
Time 0 20 40 60 80 100
Low 12 7 2 1 1 0
High 11 9 4 3 3 0
Low 12 6 0 0 0 0
High 11 10 6 4 4 0
Low 12 8 4 2 2 0
High 11 8 2 2 2 0
Low 12 7 4 3 3 0
High 11 9 2 1 1 0
E
HGSOC 1
HGSOC 2
NSCLC 1
NSCLC 2
F
G
B cells
Fibroblasts
Myeloid cells
Plasma cells
CD56dim
CD56bright
T/NK cells
Tumor
Dim1 (28.6%)
Dim2 (27.1%)
Dim1 (33.7%)
Dim2 (27.6%)
Dim1 (30.6%)
Dim2 (28.7%)
Dim1 (31.7%)
Dim2 (24.9%)
H
T cells-CD56bright
CD56bright-CD56dim
T cells-CD56dim
CD56dim-Myeloid cells
CD56dim-Fibroblast
CD56bright-Myeloid cells
CD56bright-Fibroblast
T cells-Fibroblasts
Plasma cells - Fibroblasts
Tumor - Myeloid cells
T cells-Myeloid cells
T cells - B cells
Myeloid cells-Fibroblasts
Tumor - Fibroblasts
Tumor - CD56dim
T cells-Plasma cells
CD56dim - Plasma cells
CD56bright - Plasma cells
Tumor - CD56bright
CD56bright - B cells
CD56dim - B cells
Tumor - T cells
Plasma cells - B cells
Tumor - Plasma cells
Plasma cells - Myeloid cells
Fibroblasts - B cells
Tumor - B cells
Myeloid cells - B cells
Correlation
sample
hgsoc_1_b
hgsoc_2_a
nsclc_1_b
nsclc_2_a
padj = 0.05
I
B cells
Fibroblasts
Myeloid cells
Plasma cells
T/NK cells
Tumor
LUNG
OVA
% of neighbors
CD56dimCD56bright
CD56dim CD56bright

***Supplementary Figure 8*. The interplay between CD8$^+$ T and NK cells subsets within HGSOC and NSCLC tumor samples.** (A-D) Overall survival (OS) of chemo-naïve HGSOC (n=22) (A, B) and NSCLC (n=23) (Cohorts 9 and 10) (C, D), upon stratification based on median frequency of CD8$^+$ T cells in close proximity (<10 μm) to CD57$^+$CD3$^-$ and NKG2A$^+$CD3$^-$ NK cells. Survival curves were estimated by the Kaplan–Meier method, and differences between groups were evaluated using the log-rank test. The number of patients at risk is reported. (E) Spatial organization of cells in the HGSOC and NSCLC samples as determined by Xenium in situ (Cohorts 9 and 10). Niches were defined based on the composition of 30 nearest spatial neighbors using the *BuildNicheAssay* function in *Seurat*. (F) Bar plots showing cell type compositions within the niches presented in E. (G) Principal component analysis (PCA) of niche distributions across cell types. (H) Pairwise correlations of niche distributions between cell types. Each colored dot represents one sample; large dots indicate mean values with 5–95% confidence intervals. Cell type pairs are ordered by mean correlation. Dashed line marks the significance threshold (adjusted $p = 0.05$). (I) Spatial neighbors of NK^{dim} and NK2^{bright} cells. Each dot represents the frequency of a given cell type within 50 μm of an NK1 or NK2 cell centroid. NK1–NK2 pairs from the same sample are connected by lines.

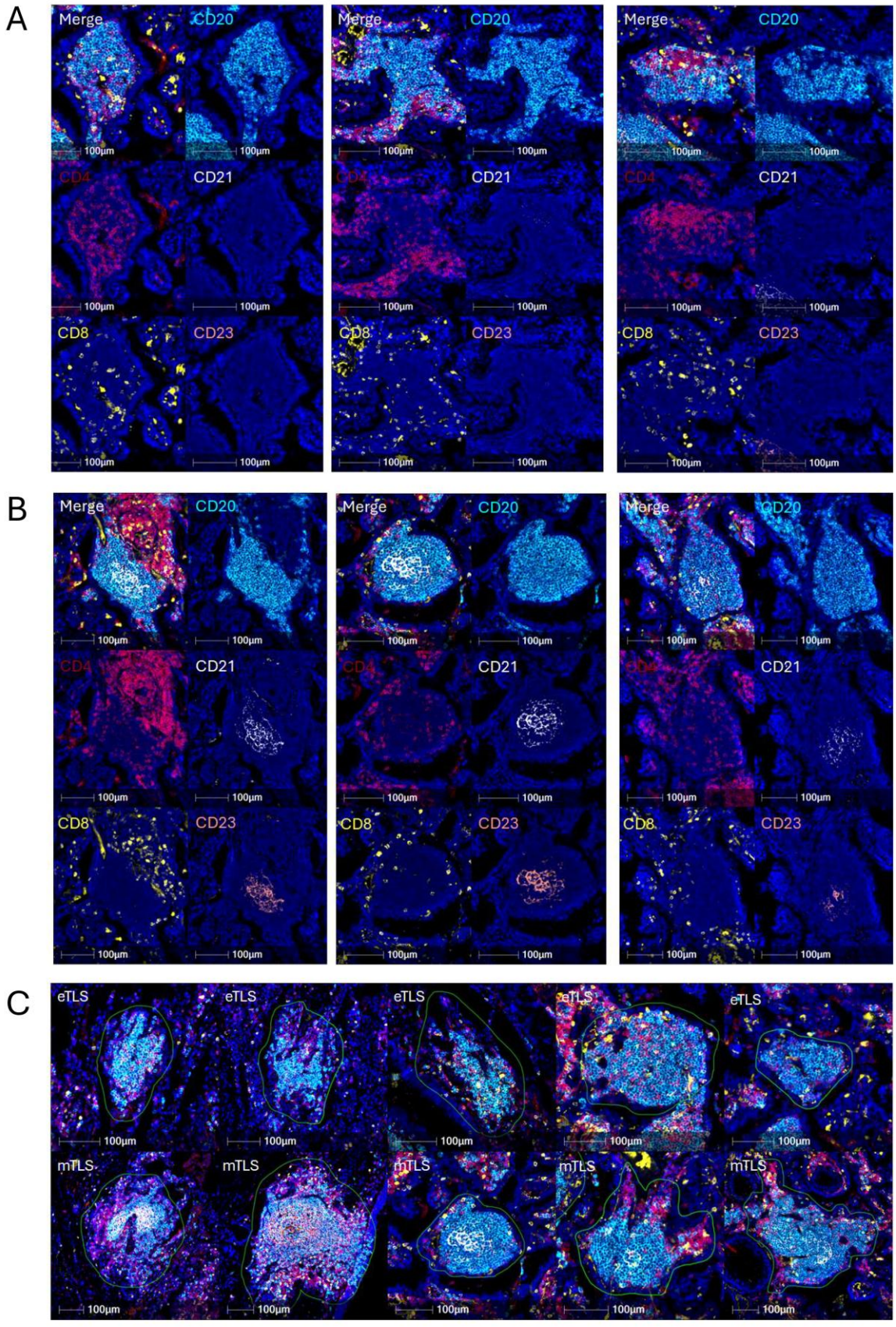

Supplementary Figure 9. **Spatial distribution of eTLS and mTLS.** (A, B) Representative images of eTLS (A) and mTLS (B) using immunofluorescence staining of CD4, CD8, CD20, CD21, CD23, DC-LAMP and GZMB (Immunofluorescence panel 2). (C) Representative image of TLS area quantification in HALO software. Scale bar 100 µm.

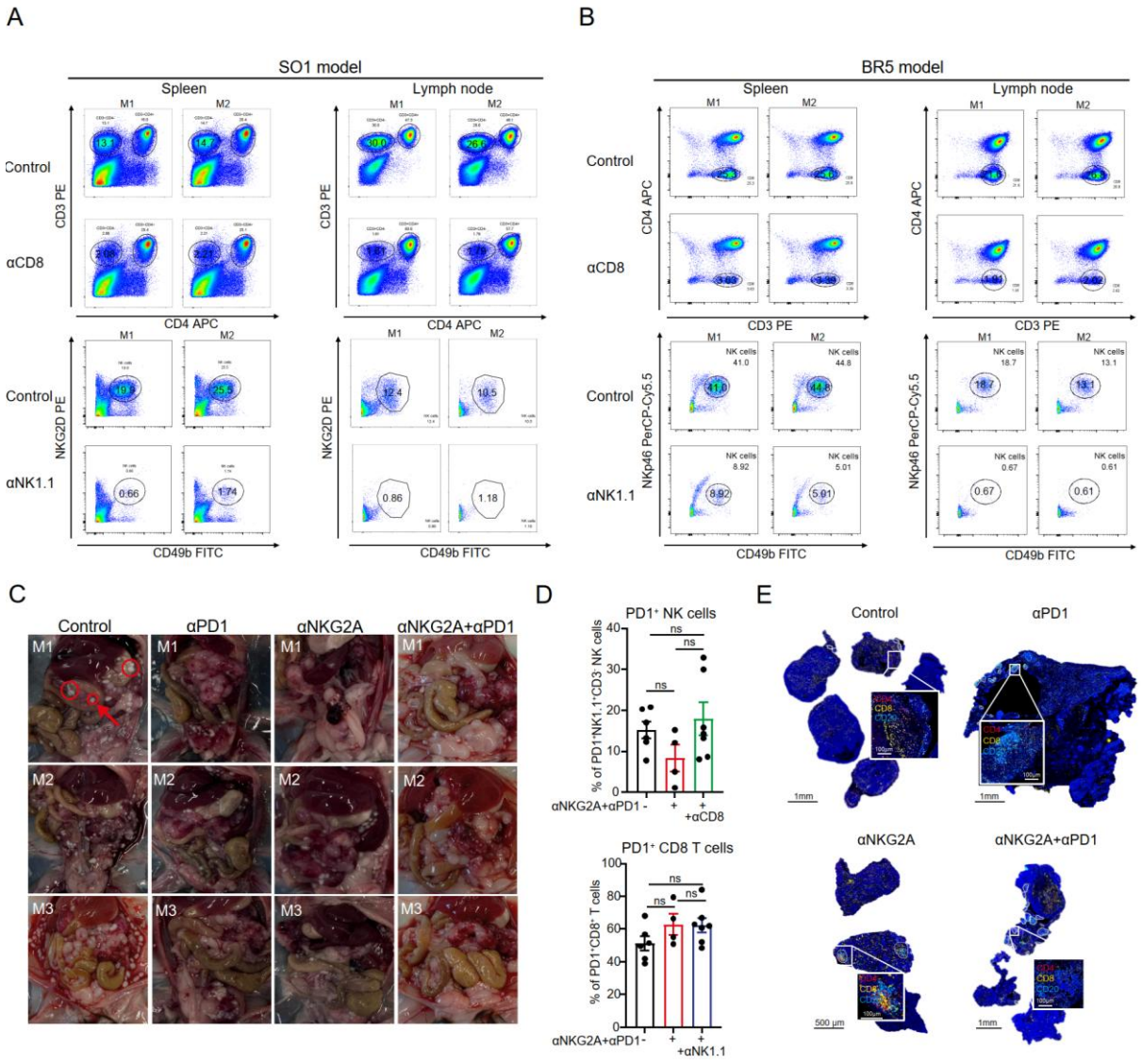

Supplementary Figure 10. **The impact of NK cell and CD8$^+$ T cell depletion on anti-tumor immunity development in mouse models of ovarian carcinoma.** (A, B) Representative dot plots of CD8$^+$ T cells and NK1.1$^+$CD3$^-$CD45$^+$ NK cells in spleen and lymph nodes before and after aNK1.1 and aCD8 depletion in SO1 (A) and BR5 (B) experimental models. (C) Representative necropsy images showing macroscopic peritoneal metastatic lesions from three individual SO1-bearing mice (indicated as M1–M3) treated with αNKG2A, αPD1, or the combination therapy. Red arrows indicate metastatic tumor nodules. (D) Bar plot showing percentage of PD1$^+$CD45$^+$CD3$^-$NK1.1$^+$ NK cells and percentage of PD1$^+$CD8$^+$ T cells after combined αPD1 and αNKG2A therapy following CD8$^+$ T cells (αCD8) and NK cells (αNK1.1) depletion, respectively, determined by flow cytometry. Mean and SEM are shown. Statistical significance was calculated by two-sided Mann–Whitney U test. *p* values are indicated. (E) Representative immunostaining for CD4, CD8 and CD20 showing distribution of tertiary lymphoid structures (TLS) within control, αPD1, αNKG2A and combined αPD1+αNKG2A treated SO1 ovarian tumors. Scale bars 100µm, 500µm and 1mm.

A

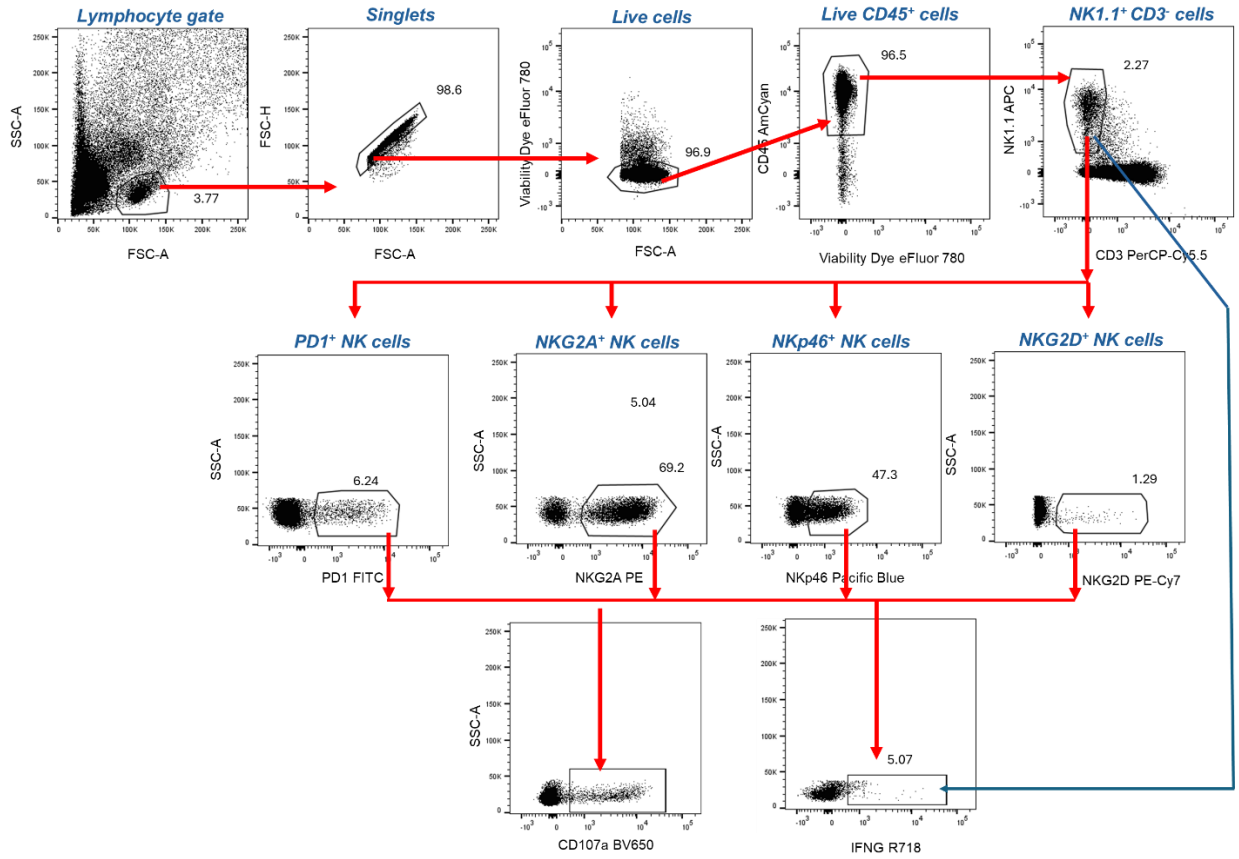
Lymphocyte gate
SSC-A
FSC-A
3.77
Singlets
FSC-H
FSC-A
98.6
Live cells
Viability Dye eFluor 780
FSC-A
96.9
Live CD45+ cells
CD45 AmCyan
Viability Dye eFluor 780
96.5
NK1.1+ CD3- cells
NK1.1 APC
CD3 PerCP-Cy5.5
2.27
PD1+ NK cells
SSC-A
PD1 FITC
6.24
NKG2A+ NK cells
SSC-A
NKG2A PE
5.04
69.2
NKp46+ NK cells
SSC-A
NKp46 Pacific Blue
47.3
NKG2D+ NK cells
SSC-A
NKG2D PE-Cy7
1.29
SSC-A
CD107a BV650
SSC-A
IFNG R718
5.07

B

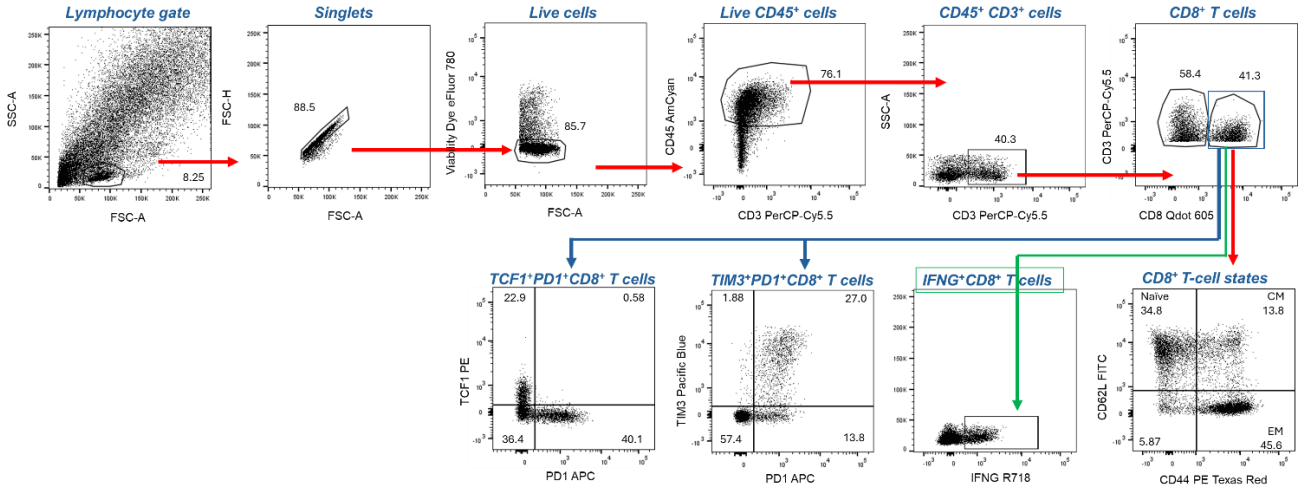
Lymphocyte gate
SSC-A
FSC-A
8.25
Singlets
FSC-H
FSC-A
88.5
Live cells
Viability Dye eFluor 780
FSC-A
85.7
Live CD45+ cells
CD45 AmCyan
CD3 PerCP-Cy5.5
76.1
CD45+ CD3+ cells
SSC-A
CD3 PerCP-Cy5.5
40.3
CD8+ T cells
CD3 PerCP-Cy5.5
CD8 Qdot 605
58.4
41.3
TCF1+PD1+CD8+ T cells
TCF1 PE
PD1 APC
22.9
0.58
36.4
40.1
TIM3+PD1+CD8+ T cells
TIM3 Pacific Blue
PD1 APC
1.88
27.0
57.4
13.8
IFNG+CD8+ T cells
IFNG R718
CD8+ T-cell states
CD62L FITC
CD44 PE Texas Red
Naïve
34.8
CM
13.8
5.87
EM
45.6

C

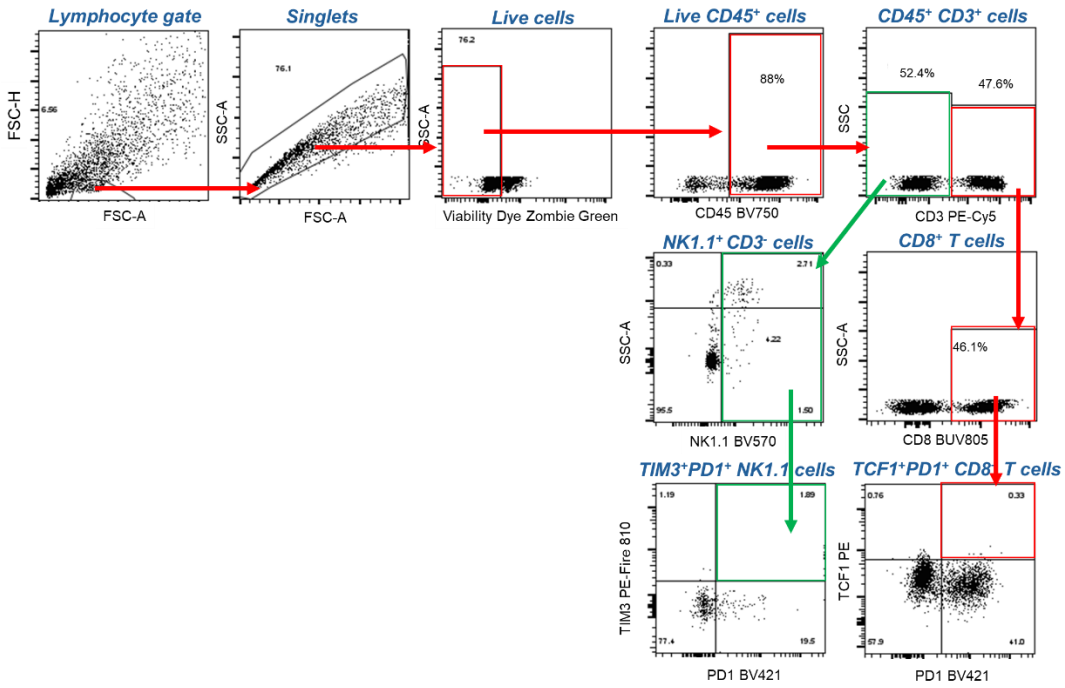

Supplementary Figure 11. **Gating strategy in murine tumor samples.** (A) Detection of relative numbers of PD1$^+$, NKG2A$^+$, NKp46$^+$ and NKG2D$^+$ NK1.1$^+$CD3$^-$CD45$^+$ NK cells; frequency of IFNG$^+$ and CD107a$^+$ PD1$^+$, NKG2A$^+$, NKp46$^+$ and NKG2D$^+$ NK1.1$^+$CD3$^-$CD45$^+$ NK cells, respectively. This gating strategy supports analyses presented in Fig. 5H-L and in Fig. 6F-G, I-J. (B) Detection of relative numbers of PD1$^+$, TCF1$^+$PD1$^+$, TIM3$^+$PD1$^+$ CD8$^+$ T cells and frequency of CD44$^+$CD62L$^-$ effector memory (T_{EM}), CD44$^+$CD62L$^+$ central memory (T_{CM}) and CD44$^-$CD62L$^+$ naïve (T_N) CD8$^+$ T cells. This gating strategy supports analyses presented in Fig. 5M-P and in Fig. 6C-E, H, K. (C) Detection of relative numbers of TIM3$^+$PD1$^+$NK1.1$^+$CD3$^-$CD45$^+$ NK cells and TCF1$^+$PD1$^+$ CD8$^+$ T cells. This gating strategy supports analyses presented in Fig. 6N. Percentage of cells in each gate is reported and detailed gating strategy is shown.

Supplementary Tables

Supplementary Table 1. **Gene signatures related to NK-cell activating ligands and ER stress response.** Unless specified, gene and protein nomenclature is official as per PubMed Gene (https://www.ncbi.nlm.nih.gov/gene).

Protein	Gene name	Full name
		NK cell activating ligands
CD58	*CD58*	CD58 molecule
ICAM1	*ICAM1*	intercellular adhesion molecule 1
MICA	*MICA*	MHC class I polypeptide–related sequence A
RAET1E	*RAET1E*	retinoic acid early transcript 1E
ULBP1	*ULBP1*	UL16 binding protein 1
HLAE	*HLAE*	major histocompatibility complex, class I, E
CD155	*PVR*	PVR cell adhesion molecule
		ER stress response
CHOP	*DDIT3*	DNA damage inducible transcript 3
GRP94	*HSP90B1*	heat shock protein 90 beta family member 1
BIP	*HSPA5*	heat shock protein family A (Hsp70) member 5
ATF4	*ATF4*	activating transcription factor 4
ATF6	*ATF6*	activating transcription factor 6
DR5	*TNFRSF10B*	TNF receptor superfamily member 10b
CANX	*CANX*	calnexin
eIF2α	*EIF2S1*	eukaryotic translation initiation factor 2 subunit alpha
PERK	*EIF2AK3*	eukaryotic translation initiation factor 2 alpha kinase 3
IRE1α	*ERN1*	endoplasmic reticulum to nucleus signaling 1
GADD34	*PPP1R15A*	protein phosphatase 1 regulatory subunit 15A

Supplementary Table 2. **Gene signatures related to NK1, 2 and 3 clusters.** Unless specified, gene and protein nomenclature is official as per PubMed Gene (https://www.ncbi.nlm.nih.gov/gene).

Protein	Gene name	Full name
		NK1 cells gene signature
CD16	*FCGR3A*	Fc gamma receptor IIIa
CD160	*CD160*	CD160 molecule
CLN10	*CTSD*	cathepsin D
CCL4	*CCL4*	C-C motif chemokine ligand 4
GPR56	*ADGRG1*	adhesion G protein-coupled receptor G1
CD38	*CD38*	CD38 molecule
CD3 ZETA	*CD247*	CD247 molecule
GST2	*CHST2*	carbohydrate sulfotransferase 2
CX3CR1	*CX3CR1*	C-X3-C motif chemokine receptor 1
CD161	*KLRB1*	killer cell lectin like receptor B1
CD306	*LAIR2*	leukocyte associated immunoglobulin like receptor 2
FSTL2	*IGFBP7*	insulin like growth factor binding protein 7
DDX	*AKR1C3*	aldo-keto reductase family 1 member C3
FGFBP2	*FGFBP2*	fibroblast growth factor binding protein 2
TTNAP	*MYOM2*	myomesin 2
CLIC3	*CLIC3*	chlorin intracellular channel 3
GZMB	*GZMB*	granzyme B
PRF1	*PRF1*	perforin 1
CD23	*FCER1G*	Fc epsilon receptor Ig
NKG7	*NKG7*	natural killer cell granule protein 7
SPON2	*SPON2*	spondin 2
		NK2 cells gene signature
TNFC	*LTB*	lymphotoxin beta
AP-1	*FOS*	Fos proto-oncogene
IL2RB	*IL2RB*	interleukin 2 receptor B
IFITM3	*IFITM3*	interfreron induced transmembrane protein 3
CLP	*COTL1*	coactosin like F-actin binding protein 1
IL7R	*IL7R*	interleukin 7 receptor
AGM7	*PIK3R1*	phosphoinositide-3-kinase regulatory subunit 1
AREG	*AREG*	amphiregulin
BRF2	*ZFP36L2*	ZFP36 like 2 zinc finger CCCH-type
PAC-1	*DUSP2*	dual specificity phosphatase 2
CD44	*CD44*	CD44 molecule
CD62L	*SELL*	selectin L
EBI2	*GPR183*	G protein-couplet receptor 183
CMC1	*CMC1*	C-X9-C motif containing 1
NKG2A	*KLRC1*	killer cell lectin like receptor C1
TCF1	*TCF7*	transcription factor 7
TCTP	*TPT1*	tumor protein translationalll controlled 1
XCL2	*XCL2*	X-C motif chemokine ligand 2
XCL1	*XCL1*	X-C motif chemokine ligand 1
GZMK	*GZMK*	granzym K
CD56	*NCAM1*	neural cell adhesion molecule 1
		NK3 cells gene signature
HBA1	*HBA1*	hemoglobin subunit alpha 1
CD3G	*CD3G*	CD3 gamma subunit of T-cell receptor complex
CD3D	*CD3D*	CD3 delta subnit of T-cell receptor complex
DSTN	*DSTN*	destrin, actin depolymerizing factor
ZNF921	*ZBTB38*	zinc finger and BTB domain containing 38 Homo sapiens
CD2	*CD2*	CD2 molecule
PPDPF	*PPDPF*	pancreatic progenitor cell differentiation and proliferation factor
Blimp-1	*PRDM1*	PR domain containing 1, with ZNF domain

GAL1	*LGALS1*	galectin 1
MTS1	*S100A4*	S100 calcium binding protein A4
CD29	*ITGB1*	Integrin subunit beta 1
IL32	*IL32*	interleukin 32
VIM	*VIM*	vimentin
S100A6	*S100A6*	S100 calcium binding protein A6
ParaT	*PTMS*	parathymosin
GZMH	*GZMH*	granzym H
CD3E	*CD3E*	CD3 antigen, epsilon polypeptide
CCL5	*CCL5*	C-C motif chemokine ligand 5
NKG2C	*KLRC2*	killer cell lectin like receptor C2

Supplementary Table 3. **Gene signature related to NK-cell phenotypic and functional properties.** Unless specified, gene and protein nomenclature is official as per PubMed Gene (https://www.ncbi.nlm.nih.gov/gene).

Protein	Gene name	Full name
Cytotoxicity gene signature		
PRF1	*PRF1*	perforin 1
GZMH	*GZMH*	granzym H
GZMB	*GZMB*	granzym B
NKG7	*NKG7*	natural killer cell granule protein 7
FASLG	*FASLG*	Fas ligand
DF5L	*GSDMD*	gasdermin D
GZMA	*GZMA*	granzym A
GZMK	*GZMK*	granzym K
TRAIL	*TNFSF10*	TNF superfamily member 10
Cytokines gene signature		
FLT3LG	*FLT3LG*	fms related receptor tyrosine kinase 3 ligand
XCL2	*XCL2*	X-C motif chemokine ligand 2
XCL1	*XCL1*	X-C motif chemokine ligand 1
IFNG	*IFNG*	interferon gamma
CCL4L2	*CCL4L2*	C-C motif chemokine ligand 4 like 2
CCL4	*CCL4*	C-C motif chemokine ligand 4
CCL3	*CCL3*	C-C motif chemokine ligand 3
IL16	*IL16*	interleukin 16
CCL5	*CCL5*	C-C motif chemokine ligand 5
IL32	*IL32*	interleukin 32
Cytokine receptors gene signature		
TGFR-1	*TGFBR1*	transforming growth factor beta receptor 1
TGFR-2	*TGFBR2*	transforming growth factor beta receptor 2
TGFR-3	*TGFBR3*	transforming growth factor beta receptor 3
IL10 Receptor β	*IL10RB*	interleukin 10 receptor subunit beta
IL12 Receptor β1	*IL12RB1*	interleukin 12 receptor subunit beta 1
IL2 Receptor γ	*IL2RG*	interleukin 2 receptor subunit gamma
IL10 Receptor α	*IL10RA*	interleukin 10 receptor subunit alpha
IL18RAP	*IL18RAP*	interleukin 18 receptor accessory protein
IL18 Receptor 1	*IL18R1*	interleukin 18 receptor 1
IL2 Receptor β	*IL2RB*	interleukin 2 receptor beta
Activating receptors gene signature		
CD160	*CD160*	CD160 molecule
NKp30	*NCR3*	natural cytotoxicity triggering receptor 3
NKG2C	*KLRC2*	killer cell lectin like receptor C2
SLAMF7	*SLAMF7*	signaling lymphocyte activation molecule 7
NKG2D	*KLRK1*	killer cell lectin like receptor K1
SLAMF6	*SLAMF6*	signaling lymphocyte activation molecule 6
Inhibitory receptors gene signature		
TIM3	*HAVCR2*	Hepatitis A virus cellular receptor 2
CD158E1	*KIR3DL1*	Killer cell immunoglobulin like receptor, 3 Ig domains and long cytoplasmic tail 1
CD158A	*KIR2DL1*	Killer cell immunoglobulin like receptor, 2 Ig domains and long cytoplasmic tail 1
TIGIT	*TIGIT*	T cell immunoreceptor with Ig and ITIM domains
CD300A	*CD300A*	CD300a molecule
CD158K	*KIR3DL2*	killer cell immunoglobulin like receptor, three Ig domains and long cytoplasmic tail 2
CD158B2	*KIR2DL3*	killer cell immunoglobulin like receptor, two Ig domains and long cytoplasmic tail 3
NKG2A	*KLRC1*	killer cell lectin like receptor C1
CD161	*KLRB1*	killer cell lectin like receptor B1
SIGLEC7	*SIGLEC7*	sialic acid binding Ig like lectin

Supplementary Table 4. **The main clinicopathological characteristics of 42 chemo-naïve HGSOC (Cohort 3) and 18 neoadjuvant chemotherapy-treated HGSOC (Cohort 5) patients involved in the prospective study group.**

Variable	Cohort 3 (n=42)	Cohort 5 (n=18)
Age		
Mean Age	62	64
Range	30-78	36-77
pTNM stage		
Stage III	38 (90%)	18 (100%)
IIIA	9 (21%)	0 (0%)
IIIB	6 (14%)	3 (17%)
IIIC	23 (55%)	15 (83%)
Stage IV	4 (10%)	0 (0%)
Tumor localization		
P-TME	n=42	n=18
M-TME	n=18	n=18
Neoadjuvant chemotherapy		
CBDCA+PTX	0 (0%)	18 (100%)
3x cycles	0 (0%)	18 (100%)
4x cycles	0 (0%)	0 (0%)
Non therapy	42 (100%)	0 (0%)

Abbreviations. CBDCA, carboplatin; PTX, paclitaxel; P-TME, primary tumor samples; M-TME, metastatic tumor samples

Supplementary Table 5. **The main clinicopathological characteristics of 26 chemo-naïve NSCLC (Cohort 4) patients involved in the prospective study group.**

Variable	Cohort 4 (n=26)
Age	
Mean Age	67
Range	39-81
Stage	
Stage IA	3 (12%)
Stage IB	6 (23%)
Stage IIB	6 (23%)
Stage IIIA	11 (42%)
Histology	
ADC	16 (61%)
SCC	5 (19%)
LCC	3 (12%)
ADC/LCC	2 (8%)
Sex	
Female	4
Male	20
NA	2

Abbreviations. ADC, adenocarcinoma; SCC, squamous cell carcinoma; NA, not available

Supplementary Table 6. **The main clinicopathological characteristics of 24 HGSOC (Cohort 9) and 24 NSCLC (Cohort 10) patients from the retrospective study group.**

Database lock for this study was performed on 1 January 2023 to finalize the dataset for analysis.

Variable	Cohort 9 (n=24 HGSOC)
Age	
Mean Age	58
Range	38-78
Sex	
Female (F)	24 (100%)
Histology	
HGSOC	24 (100%)
pTNM stage	
Stage III	21 (87,5%)
IIIA	1 (4%)
IIIB	3 (12.5%)
IIIC	17 (71%)
Stage IV	3 (12.5%)
Debulking	
R0	9 (37.5%)
R1	1 (4%)
R2	14 (58.5%)
Tumor localization	
P-TME	24 (100%)
Vital status of patients	
Alive	7 (29%)
Death	17 (71%)

Variable	Cohort 10 (n=24 NSCLC)
Age	
Mean Age	68
Range	50-78
Sex	
Female (F)	11 (46%)
Male (M)	13 (54%)
Histology	
ADC	24 (100%)
pTNM stage	
Stage III	24 (100%)
IIIA	14 (58%)
IIIB	10 (42%)
Tumor localization	
P-TME	24 (100%)
Vital status of patients	
Alive	11 (46%)
Death	13 (54%)

Supplementary Table 7. **Antibodies and detection systems used for immunohistochemistry and immunofluorescence staining.**

Parameter	Source	Producer	Clone	Detection system	Revelation	Dilution	Incubation time [min]
Immunohistochemistry							
CD3	rabbit	Abcam	SP162	Impress HRP anti-rabbit IgG (Peroxidase) Polymer Detection kit	AEC+ substrate Chromogen system	1:100	60
CD4	rabbit	LSBio	RBT-CD4	Impress HRP anti-rabbit IgG (Peroxidase) Polymer Detection kit	DAB+ substrate Chromogen system	1:50	120
CD4	rabbit	Abcam	EPR19514	Impress HRP anti-rabbit IgG (Peroxidase) Polymer Detection kit	AEC+ substrate Chromogen system	1:150	60
CD8	rabbit	Abcam	CAL38	Impress EXCEL Amplified anti-rabbit IgG kit; Impress HRP anti-goat IgG (peroxidase) Polymer Detection kit	ImmPACT DAB EqV Substrate Kit	1:250	60
CD20	rabbit	Abcam	SP32	Impress HRP anti-rabbit IgG (Peroxidase) Polymer Detection kit	AEC+ substrate Chromogen system	1:100	60
CD21/CR2	mouse	Cell signalling	2G9	Impress HRP anti-mouse IgG (Peroxidase) Polymer Detection kit	AEC+ substrate Chromogen system	1:50	60
CD23	rabbit	Abcam	SP23	Impress HRP anti-rabbit IgG (Peroxidase) Polymer Detection kit	AEC+ substrate Chromogen system	1:200	60
CD45	mouse	RD Systems	MAB1430 2	poly-HRP-conjugated sec.Ab goat anti-mouse + Biotin XX Tyramide reagent + Streptavidin-HRP	AEC+ substrate Chromogen system	1:100	60
CD57	mouse	Abcam	NK/804	Impress HRP anti-mouse IgG (Peroxidase) Polymer Detection kit	AEC substrate system	1:50	120
HLA-E	mouse	Invitrogen	MEM-E/06	Impress EXCEL Amplified anti-mouse IgG kit;Impress HRP anti-goat IgG (peroxidase) Polymer Detection kit	ImmPACT DAB EqV Substrate Kit	1:100	60
NCR1	rabbit	Abcam	EPR23097-35	Impress HRP anti-rabbit IgG (Peroxidase) Polymer Detection kit	AEC substrate system	1:500	60
NKG2A	rabbit	Abcam	EPR23737-127	Impress HRP anti-rabbit IgG (Peroxidase) Polymer Detection kit	AEC substrate system	1:500	60
NKp46	rabbit	Abcam	EPR22403-57	poly-HRP-conjugated sec.Ab goat anti-rabbit + Biotin XX Tyramide reagent + Streptavidin-HRP	AEC substrate system	1:100	60
PanCK	mouse	Abcam	AE1/AE3	Impress HRP anti-mouse IgG (Peroxidase) Polymer Detection kit	AEC substrate system	1:100	60
Immunofluorescence		**Panel 1+2**					
CD8	rabbit	Abcam	SP16	poly-HRP-conjugated sec.Ab goat anti-rabbit	Alexa Fluor™ 594 Tyramide reagent	1:60	90
CD20	mouse	Dako	L26	goat anti-mouse IgG (H+L cross absorbed secondary antibody A750	NA	1:300	60
DC-LAMP	rat	Dendritics	1010E1.01	Immpress -HRP anti-rat IgG polymer	Alexa Fluor™ 546 Tyramide reagent	1:350	overnight
GZMB	rabbit	Abcam	EPR8260	poly-HRP-conjugated sec.Ab goat anti-rabbit	Alexa Fluor™ 488 Tyramide reagent	1:250	60
	Panel 3						
NKG2A	Rabbit	Abcam	EPR23737-127	Opal Anti-Ms + Rb HRP	Opal Polaris 570	1:400	90
CD8	Rabbit	Abcam	SP16	Opal Anti-Ms + Rb HRP	Opal Polaris 480	1:50	90
CD3	Rabbit	Abcam	SP162	Opal Anti-Ms + Rb HRP	Opal Polaris 690	1:100	60
PanCK	Mouse	Abcam	AE1/AE3	Opal Anti-Ms + Rb HRP	Opal Polaris 620	1:200	60

***Supplementary Table 8*. The list of antibodies used for flow cytometry.**

Parameter	Source	Producer	Clone	Catalog number	Fluorochrome	Dilution
Annexin V	NA	Exbio	NA	EXB0027	PE	2:100
CALR	mouse	Enzo Life eSciences, Ing	FMC75		APC	2.4:100
CD3	mouse	Exbio	MEM-57	A7-202-T100	A700	5:100
CD3	rat	BioLegend	17A2	100218	PerCP Cy 5.5	1:100
CD3	rat	Invitrogen	17A2	15-0032-82	PE-Cy5	0.125:100
CD3	mouse	BioLegend	SK7	344861	Spark NIR 685	5:100
CD8	mouse	BD Biosciences	RPA-T8	560774	HV 500	5:100
CD8a	rat	BD BioSciences	53-6.7	563152	BV605	1:100
CD8a	rat	BD Biosciences	53-6.7	612898	BUV805	0.25:100
CD8a	mouse	BioLegend	RPA-T8	301026	Pacific Blue	0.5:100
CD16	mouse	BioLegend	3G8	302012	APC	5:100
CD16/CD32 (Fc Block)	rat	BD Biosciences	2.4G2	553142	NA	1:20
CD44	rat	BD Biosciences	IM7	562464	PE-CF594	1:100
CD45	mouse	BD Biosciences	HI30	560777	HV500	5:100
CD45	mouse	Thermo Fisher Scientific	HI30	MHCD4517	PE-Texas Red	6:100
CD45	rat	Invitrogen	30-F11	69-0451-82	eF506	0.5:100
CD45	rat	BD Biosciences	30-F11	746947	BV750	0.125:100
CD45	mouse	BioLegend	HI30	304095	SparkPLUS UV395	0.25:100
CD56	mouse	BioLegend	MEM-188	304626	PerCP Cy5.5	6:100
CD56	mouse	BioLegend	HCD-56	318328	BV421	6:100
CD56	mouse	BioLegend	5.1H11	362554	APC-Fire 750	0.3:100
CD62L	rat	BD Biosciences	MEL/14	553150	FITC	1:100
CD107a	rat	BioLegend	1D4B	121645	BV650	0.25:100
EPCAM	mouse	BioLegend	9C4	324204	FITC	2:100
GZMB	mouse	BD Biosciences	GB11	560213	Alexa Fluor 700	0.03125:100
IFNG	rat	Invitrogen	XMG1.2	12-7311-82	PE	1:100
IFNG	rat	BD Biosciences	XMG1.2	567061	R718	0.25:100
NK1.1	mouse	BioLegend	PK136	108733	BV570	1:100
NK1.1	rat	Invitrogen	PK136	17-5941-82	APC	1:100
NK1.1	rat	Invitrogen	PK136	25-5941-82	PE-Cy7	1:100
NKG2A	mouse	BioLegend	S19004C	375108	APC	6:100
NKG2A	mouse	BioLegend	S19004C	375104	PE	6:100
NKG2A	rat	MACS Miltenyi Biotec	REA1161	130-120-371	PE	1:100
NKG2A	rat	BD Biosciences	20d5	741125	BUV496	0.25:100
NKG2A	mouse	BD Biosciences	131411	747919	BV711	2.5:100
NKG2D	rat	Invitrogen	CX5	25-5882-82	PE-Cy7	1:100

NKG2D	rat	Invitrogen	CX5	46-5882-82	PerCP-eFluor 710	1:100
NKG2D	mouse	BioLegend	ID11	320843	PE-Cy5	5:100
NKp46	mouse	BioLegend	9E2	331919	PerCP Cy5.5	2:100
NKp46	rat	BD Biosciences	29A1.4	562850	BV421	1:100
NKp46	rat	BD Biosciences	29A1.4	756928	RB744	1:100
PD1	mouse	BioLegend	EH12.2H7	329904	FITC	6:100
PD1	rat	BioLegend	RMP1-30	109112	APC	1:100
PD1	rat	BioLegend	29F.1A12	135214	FITC	1:100
PD1	rat	BD Biosciences	RMP1-30	748268	BV421	1:100
TCF1	rabbit	Cell Signaling	C63D9	2203S	NA	0.167:100
TIM3	mouse	BioLegend	F38-2E2	345006	PE	3:100
TIM3	rat	BD BioSciences	5D12/TIM3	747626	BV421	4:100
TIM3	rat	BioLegend	RMT3-23	119745	PE-Fire 810	2:100
Anti-rabbit IgG	goat	Cell Signaling	NA	79408S	PE	1:600
Fixable Viability Dye		eBioscience	NA	**65-0865-14**	eFluor780	1:2000
Fixable Dead Cell Stain		Thermo Fisher Scientific	NA	L34962	LIVE/DEAD Blue	1:500
Fixable Viability Dye		BioLegend	NA	423111	Zombie Green	1:4000

Supplementary Table 9. Flow cytometry instruments configuration.

A) BD LSRFortessa flow cytometer (BD Biosciences)
Software - BD FACSDiva 8.0.3
Configuration – 3L (B,R,V):

BD LSRFortessa				
Laser	Detector position	Filter Long Pass	Filter Band Pass	Name of the detector
Blue 488nm octagon	E	505LP	530/30	FITC
	D	550LP	575/26	PE
	C	600LP	610/20	PE-Texas Red
	B	685LP	695/40	PerCP-Cy5.5
	A	750LP	780/60	PE-Cy7
Red 640nm trigon	C		670/14	APC
	B	710LP	730/45	AlexaFluor700
	A	750LP	780/60	APC_Cy7
Violet 405nm trigon	C		450/50	PacificBlue
	B	475LP	525/50	AmCyan
	A	595LP	605/12	Qdot605

B) Cytek Aurora (Cytek) spectral cytometer
Software – SpectroFlo 3.3.0
Configuration – 5L UV-V-B-YG-R

Aurora 5L UV-V-B-YG-R			
Laser	Channel	Wavelength Start (nm)	Wavelength End (nm)
UV 355 nm	UV1	365	380
	UV2	380	395
	UV3	420	435
	UV4	435	450
	UV5	450	480
	UV6	465	480
	UV7	500	528
	UV8	528	556
	UV9	566	597
	UV10	597	628
	UV11	650	667
	UV12	677	705
	UV13	705	734
	UV14	735	765
	UV15	765	795
	UV16	795	829
Violet 405 nm	V1	420	435
	V2	436	451
	V3	451	466
	V4	466	481
	V5	498	518
	V6	516	533
	V7	533	550
	V8	571	590
	V9	588	608
	V10	605	625
	V11	651	678
	V12	678	706
	V13	706	735
	V14	735	765
	V15	765	795
	V16	795	829
	B1	498	518

Blue 488 nm	B2	516	533
	B3	533	550
	B4	571	590
	B5	588	608
	B6	605	625
	B7	652	669
	B8	669	687
	B9	688	707
	B10	707	727
	B11	728	749
	B12	749	772
	B13	772	795
	B14	795	825
Red 640 nm	R1	652	669
	R2	669	687
	R3	688	707
	R4	707	727
	R5	728	749
	R6	749	772
	R7	772	795
	R8	795	829
Yellow Green 561 nm	YG1	567	587
	YG2	588	608
	YG3	605	625
	YG4	652	669
	YG5	669	687
	YG6	688	707
	YG7	706	735
	YG8	735	765
	YG9	765	795
	YG10	795	829